Modelling multi-spectral LIDAR vegetation backscatter – assessing structural and physiological information content

Felix Morsdorf[1], Caroline Nichol[1], Timothy J. Malthus[1], Genevieve Patenaude[1] & Iain H. Woodhouse[1]

[1]School of Geosciences, University of Edinburgh, Edinburgh EH8 9XP, Scotland, UK
felix.morsdorf@ed.ac.uk

Abstract

The concept for a new multi-spectral canopy LIDAR (MSCL) instrument was tested by simulating return waveforms using models providing tree structure (TREEGROW) and leaf reflectance (PROSPECT). The proposed instrument will take measurements at four different wavelengths, which were chosen according to physiological processes altering leaf reflectance. The modelling was used to assess both the structural and physiological information content such a device could provide, especially if the normally structure-dominated return waveform would pick up small changes in reflectance at the leaf level. Multi-spectral waveforms were simulated for models of single Scots pine trees of different ages and at different stages of the growing season. It was shown that the LIDAR waveforms would not only capture the tree height information, but as would also pick up the seasonal and vertical variation of NDVI computed from two of the four MSCL wavelengths inside the tree canopy. It could be demonstrated that a new multi-wavelength LIDAR predictor variable could significantly improve the retrieval accuracy of photosynthetically active biomass opposed to using a single wavelength LIDAR alone. It remains unclear, however, if these findings would persist for forest stands; thus such experiments simulating more complex scenarios will be the next task in this modelling framework.

Keywords: LIDAR, full-waveform, modelling, multi-spectral, NDVI

1. Introduction

Understanding the dynamics of the global carbon cycle is one of the most crucial scientific and societal problems of the 21st century. A key part of this understanding is being able to measure and monitor (a) the magnitude of terrestrial carbon sinks, by mapping their horizontal and vertical structure, (b) rapid as well as long term change resulting from natural and human-induced disturbances (e.g. deforestation, fire, desertification) and (c) the subsequent recovery processes. Laser remote sensing has been widely used to infer estimates of vegetation structure and biomass (Lim and Treitz, 2004, Hyyppä et al., 2001, Patenaude et al., 2004), at various scales ranging from single-tree level (Morsdorf et al., 2004) to landscape-level depending on the application and/or LIDAR system used. For example, the LIDAR waveforms obtained by the spaceborne GLAS instrument have been successfully exploited for estimations of above ground biomass (Rosette et al., 2008). On the other hand, passive multi- and/or hyperspectral earth observations (EO) systems have been used to provide estimates of the physiological state of vegetation, including the discrimination of healthy versus stressed canopies (Nichol at al., 2000 and 2002, Malthus and Karpouzli, 2003). The combination of both approaches into an active multi-spectral LIDAR should join the capabilities of LIDAR and passive multi-spectral EO, while remedying some of their shortcomings when used on their own (Koetz et al., 2007), such as the dependency on solar illumination when using passive instruments. The aim of this modelling study is to show some of the potential advantages of a multi-spectral LIDAR for both the estimation of vegetation structure and physiology state and to feed back some insights into the constraints for the technical specifications of a prototype instrument. This will be achieved by combining a tree structural model, a leaf optical properties model and a model of the LIDAR measurement process together with auxiliary data about the typical physiological change occurring during a growing season. Our aim is to show that the MSCL would pick up both the structural and physiological change while adding explanatory value as opposed to using a single-wavelength LIDAR.

2. Methods

The modelling approach used to simulate LIDAR return waveforms in this study consists of three different models, one each for the leaf optical properties, the tree structure and the LIDAR measurement process. These different components and their inputs and outputs are described in the next three sections, followed by a description of the sensitivity experiment setup.

2.1 Leaf Optical Model

A widely used model of leaf optical properties (PROSPECT, Jacquemoud and Baret, 1990), was utilized to compute reflectance and transmission values of leaf tissue at the proposed MSCL wavelengths. PROSPECT was not explicitly designed to model needle reflectance, as it constructs the leaf from a number of parallel plates to resemble broadleaf structure. However, as was shown by Moorthy et al. (2008), inversion performance of leaf biochemical properties were just as good, if not better, using PROSPECT than the LIBERTY model (Dawson et al., 1998), which was specifically designed to model needles. PROSPECT has four main input parameters, which are leaf water and chlorophyll content, a leaf structure parameter (number of plates) and dry matter content. As we were interested in modelling the capability of detecting changes in NDVI during a growing season, we varied the chlorophyll concentrations for first and second year needles according to values measured by Moorthy et al. (2008), which are presented in Table 1. They measured the chlorophyll concentration in first and second year pine needles over four months. Chlorophyll concentration changes are quite large for first year needles and increase strictly monotonically. For second year needles, however, the increase over time is much smaller, with even a decrease from July to August. For each month, different chlorophyll values were used, leaving all other input parameters constant. Leaf water content would be expected to vary as well during a growing season, but would not affect the MSCL wavelengths, hence it was not considered here.

Table 1: Chlorophyll concentrations used for modelling pine needle reflectance as measured and published by Moorthy et al. (2008).

Measured Chlorophyll $\mu g/cm^2$	First year needles	Second year needles
June	16.67	37.5
July	22.90	43.8
August	24.52	40.5
September	29.28	42.2

The gained reflectance and transmittance values (see Figure 1) were then assigned to cylinders in the TREGROW output representing shoots. For bark and twigs, the same measured spectra of pine trees were used, as in the study of Koetz et al. (2004).

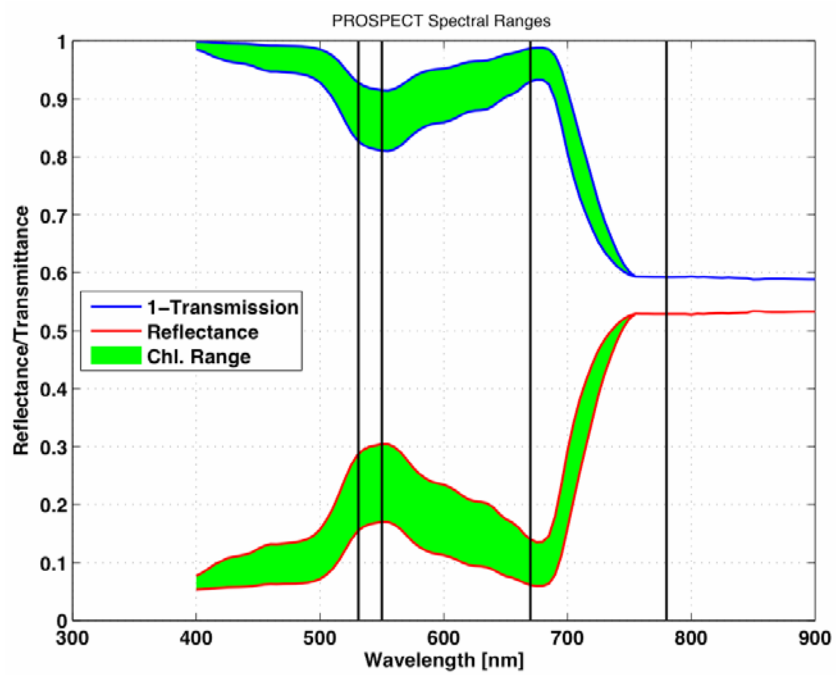

Figure1: Spectral response of leaf reflectance and transmittance as modelled by PROSPECT. The filled green areas denote the range of values spanned by the chlorophyll concentrations presented in Table 1. The vertical black lines represent the proposed MSCL wavelengths.

2.2 Tree Structural Model

We used the TREEGROW model (Leersnijder, 1992) to produce ecologically sound representations of Scots pine trees at different ages. The model has been parameterized to simulate both Scots pine and Norway spruce trees found on a test site in Sweden (see Woodhouse and Hoekmann (2000) for details). It was used previously by Woodhouse and Hoekman, (2000) and Disney et al., (2006) to model radar backscatter and passive hyperspectral signatures, respectively.

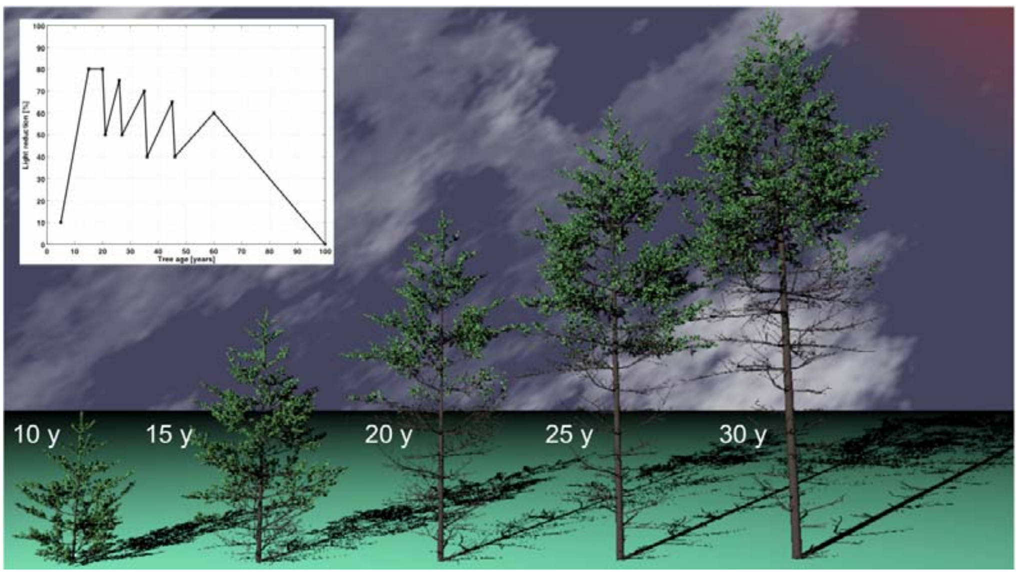

Figure 2: RGB composite rendering of the same modeled Scots pine at 5 different ages. The default TREEGROW light versus age curve (top left) was used to account for self-pruning and thinning.

The model output consists of cylinders of different sizes representing branches and shoots, with the age of each branch being stored by the model. These ages are later used to assess the development stage of each cylinder and assign reflectance values of either needles or bark to the cylinders. The cylinders representing the shoots are constructed using a semi-transparent texture in the POVRAY scene files, in order to account for shoots not being opaque (see Figure 2). A more sophisticated implementation of shoot scattering (such as described by Disney et al. (2006) or Smolander and Stenberg, (2003)) is currently in development. The default light versus age curve was used to establish thinning and pruning in the model trees, as if they would have grown in a managed forest stand, since in a later modelling stage these trees would be used to construct stand-sized forest patches.

2.3 LIDAR Measurement Model

The approach to model LIDAR returns used in this study was previously developed and published by Morsdorf et al. (2007). It builds upon the open-source ray-tracing program POVRAY, whose scene and light descriptions could be adapted to represent the LIDAR measurement process. It incorporates reflectance and transmission, and could potentially account for multiple scattering, however in the way that the model is implemented now, it only allows for single scattering. The POVRAY scene description enables the user to construct scene with arbitrary complex geometry, as such it was quite straightforward to convert the TREEGROW output into POVRAY readable files. Light distribution can be explicitly modelled across beam and thus can be set up to match those of existing LIDAR instruments. POVRAY is being used to model both a depth and an intensity image from the perspective of the emitter/receiver optics; these two images are then combined to form an approximate cross-section profile assuming the single canopy elements act as Lambertian scatterers. Following that, this cross-section is convoluted with a laser pulse of specific length and shape, again according to the specification of the prototype instrument. An illustration of the modelling process can be found in Figure 3 and the model development and validation is described in more detail in Morsdorf et al. (2007).

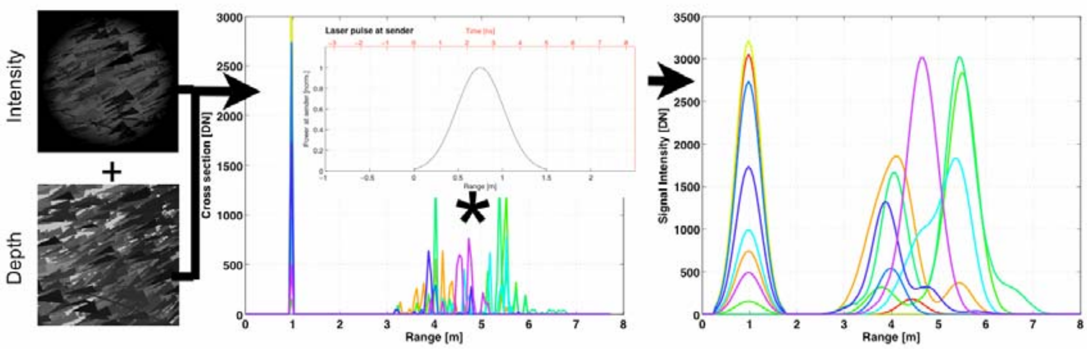

Figure 3: Illustration of waveform generation process based on intensity and depth image (left). The cross-sections (middle, at bottom) derived from these images is convoluted with a Gaussian shaped laser pulse of 5 ns length (middle, at top) to obtain the modeled LIDAR return waveforms (right).

2.4 Sensitivity study – structure and physiology

TREEGROW was used to grow the same Scots pine tree from year one to year 50, with the data being exported to a POVRAY scene file every five years. Trees aged from 10 to 50 years were used, and tree heights obtained reached from 2.5 to just over 18 meters. For each of the tree ages, four different trees had shoot reflectance assigned with reflectances based on the chlorophyll concentration for June, July, August and September. Note that first and second year needles would get different reflectance values based on their different chlorophyll concentrations. Thus, if the ratio of first to second year needles changes during maturing of the tree, it is expected to show in the modelled waveforms.

The LIDAR model was set up in a way that a single tree would be situated on a flat, horizontally levelled, spectrally homogenous plane with a spectral response of an Ericaceae understory (see Koetz et al., 2004 for details). The simulated LIDAR instrument illuminated the tree from directly above, being placed at a height of 500 m. To ensure that the total energy available to scene would not change, the beam size was fixed for all trees at different ages (and thus sizes) by making sure that the tallest tree was fitting the illuminated area. The LIDAR pulse shape was set to be of Gaussian shape and the pulse length was set to 4.75 ns (~ 1.43 m) full width at half maximum (FWHM), resembling the pulse length of the prototype instrument. For each of the four LIDAR wavelengths (531,550,670 and 780 nm) to be modelled, a separate (greyscale) POVRAY scene file had to be produced, since POVRAY only allows for one transmittance value in its RGB colour model.

3. Results and Discussion

In Figure 4, three return waveforms for 30, 40 and 50 year old trees are plotted side by side with a “real” canopy volume computed from the model tree. It was possible to differentiate between photosynthetically active canopy volume (shoots) and woody material volume (twigs, branches) in the tree model. Canopy volume was chosen as a proxy for biomass, as its computation from the model trees is straightforward and correlation with biomass should be strong and linear. The modelled waveforms exhibit the same vertical structure for all four wavelengths, but have different amplitudes. For this reason (and to save space) we present only the 780 nm waveform in Figure 4. From those waveforms, the most striking effect is the amount of smoothing due to the rather long laser pulse of 1.43 meters at FWHM; all vertical features in the canopy volume profile smaller than this distance are smoothed out. A deconvolution of the return waveform with the original laser pulse could help to reveal these features again, but for this step the original laser pulse shape needs to be known. A second feature of the return waveform is an apparent increase in tree height as well due to the convolution with the laser pulse, which makes the trees appear about 0.75-1 meter taller in the return waveform. A regression (not shown here) of LIDAR derived heights with the real heights of the model trees resulted in an R2 of 0.99, with a mean overestimation of model tree height by LIDAR by about 0.7 m, which is an effect of the convolution with the laser pulse. As with the smoothing effect before, a remedy to this with a real LIDAR system would be to know the length and the shape of the transmitted pulse and do a deconvolution. This is the reason why this information is generally provided to the user in the two commercially available single wavelength, full-waveform systems from Optech and Riegl.

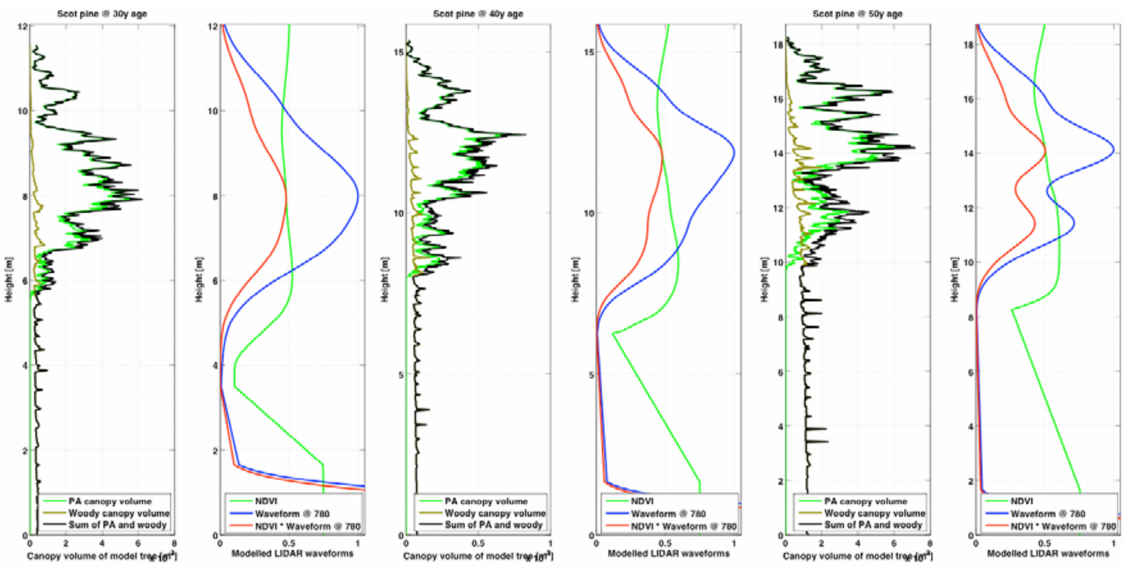

Figure 4: Canopy volume profiles and simulated LIDAR waveforms for trees of 30,40 and 50 years of age. Right panels show both photosynthetic active (PA) and woody volume components, while left panels show backscatter at 780 nm (blue), the NDVI (see Equation 1) profile (green) and a resulting waveform (red) from the multiplication of the two.

So the height information can be very well retrieved from the modelled waveforms, which is not surprising, since LIDAR remote sensing is a more or less direct measurement of canopy height. But we were also interested in assessing the physiological information content of a multiple wavelength LIDAR system. To do so, a representative measure has to be derived from the waveforms; just visually comparing the waveforms at different wavelengths would not reveal a vertical signal in the physiology. Since two of the modelled bands are enclosing the red edge (the sharp increase of reflectance/transmittance between 670 and 780 nm, see Figure 1), we are capable of computing a NDVI profile for the modelled trees according to the equation below:

$$NDVI = \frac{R_{780} - R_{670}}{R_{780} + R_{670}} \qquad (1)$$

This spectral band ratio is depicted as a green line in the right panels of Figure 4.

We were interested in quantifying the seasonal variation in this NDVI profile, which should be induced by the gain in chlorophyll concentration. In Figure 5, the vertical profiles of NDVI are depicted for selected trees; the profiles are computed for the crown extension only. Vertical extent of the tree crown was inferred manually for each tree and height thresholds for distinguishing crown material/backscatter from non-crown parts were established. NDVI increases towards the end of growing season, reaching its maximum in September. A vertical variation of NDVI is visible as well and could be explained by either the light versus age curve used to alter the ratio of “green” and “brown” canopy elements or by the ratio of first to second year needles varying vertically inside the canopy, or a combination of the two. The increase in NDVI during the growing season is largest towards the top of the tree, which is explained by the top having a larger fraction of first year needles showing a much larger variation of chlorophyll concentrations from June to September as opposed to second year needles (Table 1). However, the seasonal signal of NDVI was smaller than the vertical variation inside the tree crown.

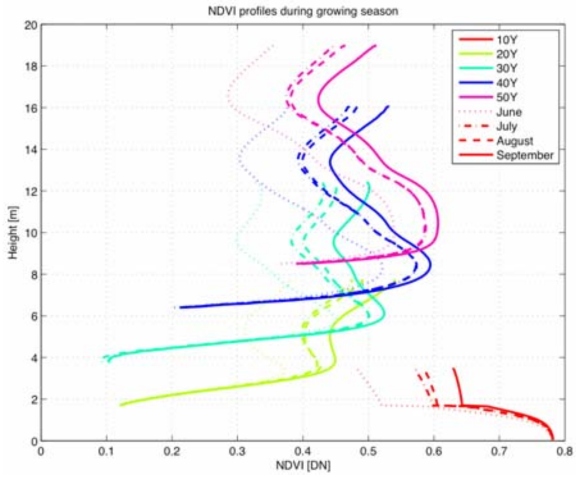

Figure 5: NDVI profiles during a growing season for model trees of different ages. Colours denote ages, line styles denote month. NDVI varies vertically and is largest towards the end of the growing season, when needles have their maximum chlorophyll concentration.

One of the main benefits for a multi-spectral LIDAR would be to more accurately provide estimates of the photosynthetic active (or "green") biomass, and thus providing a better estimate of gross primary productivity (GPP). It is well known that LIDAR instruments can provide good estimates of the vertical canopy profile, but it has not been shown in previous studies that they are able to discriminate woody and leafy canopy material, even though backscatter at 1064 nm would be of different intensity for those two vegetation components, at least in terrestrial laser scanning. However, the cumbersome calibration of airborne intensity data in vegetation and the spectrally and structural inhomogeneous canopy as illuminated by the laser footprint has yet prevented the exploitation of this information.

We computed the total canopy volume for each tree crown and correlated those with the LIDAR backscatter from the tree crown. The LIDAR backscatter was processed in two different ways, first just by summing up the backscattered energy at 780 nm (not affected by changes in chlorophyll concentration) and then by multiplying the backscatter at this wavelength with the NDVI profile to possibly retrieve a backscatter value adopted to the ratio of "green" to "brown" canopy elements. In Figure 6, these two LIDAR backscatter indicators computed for each of the nine trees are plotted over photosynthetic active canopy volume.

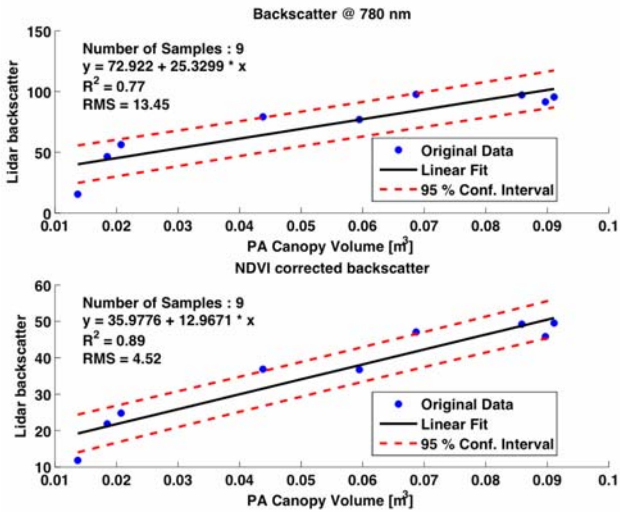

Figure 6: LIDAR backscattered energy of the tree crown versus photosynthetic active canopy volume. Using just a single, unmodified waveform (780 nm, top) will yield lower r-square than using a NDVI corrected waveform (bottom).

Using only the backscatter at 780 nm as a predictor variable, 77 % of the photosynthetic active canopy volume variation can be explained. Using the NDVI-corrected backscatter, this value increased to 89 % explained variance, revealing a potential benefit of using multiple wavelengths for estimation of photosynthetic active vegetation elements.

4. Conclusions and Outlook

The scope of this work was to illustrate the potential advantage(s) and data products of a multi-spectral canopy LIDAR (MSCL) in a modelling study. Using a tree structural model and a model of leaf optical properties, we were able to simulate multi-spectral return waveforms for Scots pine trees of different ages (thus heights) and different physiological states during a growing season. It was possible to pick up both the signal of tree growth (height evolution) and the change in chlorophyll content over a growing season by computing NDVI profiles of the trees. NDVI would vary vertically inside the tree crown to a larger extent than its seasonal cycle, with the largest seasonal variations being in the top part of the tree. The first year needles, that are abundant at the top of the tree, can explain this, since they show a much stronger seasonal variation of chlorophyll content. A new multi-spectral LIDAR predictor variable for photosynthetic active canopy elements was defined by multiplying the NDVI profile and the backscatter profile at the reference wavelength of 780 nm. This predictor variable explained a larger percentage of photosynthetic active canopy volume variation than a single wavelength alone was able to. However, it remains unclear whether this finding will persist as well in modelled forest stands, as opposed to modelled measurements of single isolated trees as done in this study. The modelling work presented in this paper is just the first of a whole set of modelling experiments undermining the concept of a multi-spectral LIDAR instrument. Further tests are going to be carried out with simulated stands constructed of TREEGROW trees of different ages, including a spectrally different understory layer and topographic undulations. Ultimately, these experiments will help explaining variations in waveforms as captured by a prototype instrument and lead to undermining the potential of future spaceborne missions with multi-spectral canopy LIDAR instruments.

References

Dawson, T. P., Curran, P. J. and Plummer, S. E., 1998. LIBERTY--Modeling the Effects of Leaf Biochemical Concentration on Reflectance Spectra. *Remote Sensing of Environment*, 65, 50-60.

Disney, M., Lewis, P. & Saich, P., 2006. 3D modelling of forest canopy structure for remote sensing simulations in the optical and microwave domains *Remote Sensing of Environment,* 100, 114-132.

Hyyppä, J., Kelle, O., Lehikoinen, M. and Inkinen, M., 2001. A segmentation-based method to retrieve stem volume estimates from 3-d tree height models produced by laser scanners. IEEE Transactions on Geoscience and Remote Sensing, 39, 969-975.

Jacquemoud, S. and Baret, F., 1990. PROSPECT: A model of leaf optical properties spectra Remote Sensing of Environment, 34, 75-91.

Koetz, B., Schaepman, M., Morsdorf, F., Itten, K. and Allgöwer, B., 2004. Radiative Transfer Modeling within a Heterogeneous Canopy for Estimation of Forest Fire Fuel Properties Remote Sensing of Environment, 2004, 92, 332-344.

Koetz, B., Sun, G., Morsdorf, F., Ranson, K., Kneubuhler, M., Itten, K. and Allgöwer, B., 2007. Fusion of imaging spectrometer and LIDAR data over combined radiative transfer models for forest canopy characterization. Remote Sensing of Environment, 106, 449-459.

Leersnijder, R.P., 1992. PINOGRAM: a pine growth area model. Wageningen Agricultural University, The Netherlands.

Lim, K. and Treitz, P., 2004. Estimation of aboveground forest biomass using airborne scanning discrete return LIDAR in Douglas-fir. In: M. Theis, B. Koch, H. Spiecker, H. Weinacker (Eds.). *Proceedings of ISPRS working group VIII/2 "Laser-Scanners for Forest and Landscape Assessment"*. Freiburg, University of Freiburg: 149-152.

Malthus, T.J. and Karpouzli, E. (2003). Integrating field and high spatial resolution satellite based methods for monitoring shallow submersed aquatic habitats in the Sound of Eriskay, Scotland, UK. *Int. Jour. of Remote Sensing*, 24(13):2585-2593.

Moorthy, I., Miller, J. R. and Noland, T. L., 2008. Estimating chlorophyll concentration in conifer needles with hyperspectral data: An assessment at the needle and canopy level *Remote Sensing of Environment,* , In Press, Corrected Proof.

Morsdorf, F., Meier, E., Kötz, B., Itten, K. I., Dobbertin, M. and Allgöwer, B., 2004. LIDAR-based geometric reconstruction of boreal type forest stands at single tree level for forest and wildland fire management *Remote Sensing of Environment*, 3, 353-362.

Morsdorf, F., Frey, O., Koetz, B. and Meier, E., 2007. Ray Tracing for Modeling of Small Footprint Airborne Laser Scanning Returns, *International Archives of Photogrammetry and Remote Sensing Volume XXXVI*, Part 3 / W52, 294-299.

Nichol, C. J., Grace J. et al. (2000). Remote sensing of photosynthetic light use efficiency of boreal forest. *Agricultural and Forest Meteorology* 101 : 131-142.

Nichol C. J., Grace J. et al. (2002). Remote sensing of photosynthetic light use efficiency of a Siberian boreal forest. *Tellus* 54B: 677-687.

Patenaude, G., Milne, R. H. R., Gaveau, D., Briggs, B. & Dawson, T., 2004. Quantifying forest above ground carbon content using LiDAR remote sensing. *Remote Sensing of Environment*, 93, 368-380.

Rosette, J., North, P. and Suarez, J., 2008. Vegetation height estimates for a mixed temperate forest using satellite laser altimetry. *International Journal of Remote Sensing*, 29, 1475-1494.

Smolander, S. and Stenberg, P., 2003. A method to account for shoot scale clumping in coniferous canopy reflectance models. *Remote Sensing of Environment,* 88, 363-373.

Woodhouse, I.H. and Hoekman, D.H., 2000. Radar modelling of coniferous forest using a tree growth model. *International Journal of Remote Sensing*, 21,8,1725-1737.